Assessment of Mechanisms of HDO-AntimiR by Molecular Dynamics Simulation

Kazutaka Nishina
Tokyo Medical and Dental University
Rintaro Iwata Hara
Tokyo Medical and Dental University
Satoru Fukuhara
University of Tokyo
Kotaro Yoshioka
Tokyo Medical and Dental University
Takanori Yokota
Tokyo Medical and Dental University
Yasushi Shibuta (shibuta@material.t.u-tokyo.ac.jp)
University of Tokyo

Research Article

Keywords: Assessment of mechanisms, HDO-antimiR, molecular dynamics simulation, DNA/RNA heteroduplex oligonucleotide-based antimiR (HDO-antimiR)

Posted Date: November 1st, 2021

DOI: https://doi.org/10.21203/rs.3.rs-1019132/v1

Abstract

Recently, we found DNA/RNA heteroduplex oligonucleotide-based antimiR (HDO-antimiR) can more efficiently inhibit the target miRNA than conventional antimiR after its cellular uptake. But the mechanism of HDO-antimiR about the target-silencing is unknown. We here tried to elucidate the interaction mechanism of HDO-antimiR to miRNA using molecular dynamics (MD) simulation. When interaction of the conventional antimiR or HDO-antimiR and the target miRNA was simulated, they combined with each other in various forms. In the hydrogen bond analyses, base site of the antimiR formed hydrogen bond with miRNA. On the other hand, phosphate site of the HDO-antimiR formed hydrogen bond with miRNA. These results suggested that there were differences about the binding mechanisms between antimiR and HDO-antimiR to the target miRNA. In particular, there was a difference in the binding site between antimiR and HDO-antimiR. Additionally, it was found that guanine in the miRNA is mainly involved in the binding to the antimiR or HDO-antimiR. MD simulation method is useful in understanding the mechanism of oligonucleotide therapeutics.

Introduction

MicroRNA (miRNA), which is one of the short endogenous RNAs, regulates various biological phenomena by suppressing more than 100 types of messenger RNA (mRNA)[1]. In recent years, it has been reported that abnormalities in miRNA expression and function are associated with various diseases such as cancer and intractable neurological diseases[2,3]. Therefore, miRNA as a biomarker for diagnosing various diseases centering on cancer has already been clinically applied, and miRNA itself has been given particular importance as a therapeutic target molecule. One of the most promising methods for controlling miRNA is the use of antimiR, a nucleic acid drug that specifically binds to miRNA via Watson-Crick base pairing by hydrogen bond and suppresses its function[4]. AntimiR consists of a single-stranded oligonucleotide which is chemically modified to improve its stability and affinity to its target miRNA. However, the silencing efficacy *in vivo* of antimiR is inadequate for clinical application and molecular design of antimiR for efficient silencing *in vivo* remains limited.

We have developed a novel molecular design of nucleic acid drugs, heteroduplex oligonucleotide (HDO) consisting of antisense oligonucleotide (ASO) targeting mRNA and its complementary RNA (cRNA)[5], and HDO greatly improves the silencing activity of conventional single-stranded ASO at the hepatocyte[6], brain microvascular endothelial cells[7] and brain[8,9] *in vivo*. Next, we designed double-stranded HDO-antimiR which comprises an antimiR strand and its cRNA-strand[10,11]. HDO-antimiR also showed the improvement of its target miRNA control ability and the avoidance of toxicity. Interestingly, while the conventional single-stranded antimiR binds directly to the target miRNA and suppresses its function on a one-to-one basis, HDO-antimiR not only binds to but also degrades the therapeutic target miRNA. However, the mechanism by which HDO-antimiR affects target miRNAs has not been elucidated. Also, traditional single-stranded antimiR is thought to form Watson-Crick base pairs with the target miRNA, whereas HDO-antimiR already forms such base pairs with the complementary RNA strand. Therefore, it is unclear in

detail how antimiR binds the target miRNA since it is not straightforward to observe such a dynamic process directly from experimental approach. To this end, molecular dynamics (MD) simulation is a powerful tool, which can handle the motion of all atoms at finite temperature directly[12]. Especially, it is an advantage of the MD simulation over static energy calculations that the steric effect can be treated inherently in the simulation since it is one of key factors to determine the interaction between nucleic acids[13] including miRNA and antimiR.

In this study, we attempted to elucidate the binding mechanism of antimiR by introducing a molecular dynamics simulation method together with the target miRNA and analyzing its operation for antimiR and HDO-antimiR.

Methods

Building and generation of models

AntimiR and HDO-antimiR containing chemically modified nucleotides were designed to target miRNA (miR122 or miR21) based on a previous report[10] and built by using Nucleic Acid Builder (NAB) tool of AMBER[14,15]. The force field (FF) parameters for the two modified nucleic acids, locked nucleic acid (LNA) and phosphorothioate (PS) bond, were available on a previous report[16]. Although each PS linkage is chiral and the chirality is known to influence the potency and safety of ASO[17,18], we used only *S*p-PS linkage in this study. The index for each atom assigned by AMBER is shown in Supplementary Figure 7. The individual modifications and sequences of the nucleic acids are shown in Table 1.

The frcmod files and lib files have been generated and have been used to build the antimiR/HDO-antimiR and target miRNA sequences for running MD simulations. Distance and angle between antimiR/HDO-antimiR and target miRNA were set using Python program.

Molecular dynamics protocol

The MD simulations were carried out using AMBERTools20 program. All the systems were neutralized by adding K^+ counter ions and solvated with TIP3P water box. All the systems were minimized by using the steepest descent method for 2000 steps. Then the systems were heated from 0 to 310 K in 20 psec. Initial structure of miRNA and antimiR or HDO-antimiR are shown in Figure 1 and Supplementary Figures 1 and 2. Followed by these steps, MD simulations were carried out for 5 nsec. MD integration was carried out using a 1 fsec time step. The pairlist was updated at every 1000 steps. Constant pressure (1 atm) and temperature (310 K) were maintained throughout the production simulation run.

All the data was collected on 1-picosecond snapshots of simulation data. The trajectories and structures were visualized using VMD. The PTRAJ module of AmberTools20 was used to measure the distance between geometric center of the sequence of miRNA and antimiR. The number of hydrogen bonds was calculated using VMD program. A distance shorter than 3 Å indicates that a hydrogen bond is formed

between the atoms of the antimiR or HDO-antimiR and miRNA are considered to be paired. All data represent mean ± s.e.m.

Results

Binding of antimiR or HDO-antimiR and miRNA from 20 Å away

At first, the distance between the antimiR or HDO-antimiR and the miRNA was fixed at 20 Å in initial state, and the angles were set in 8 directions at horizontal section of helix at 45° interval to consider the effect of initial configuration on the interaction (Figure 1, Supplementary Figures 1 and 2). Molecular simulations were performed 8 times (miR122) or 4 times (miR21) at each angle. We categorized the patterns of interaction between antimiR and miRNA as follows; Separated (no interaction), One-point interaction, Two-point interaction, Multiple-point interaction (more than two-point interaction).

As a result of simulation, all the four patterns were observed in both antimiR and HDO-antimiR (Figure 2). Then we investigated how the bonds occurred in patterns of Two-point or Multiple-point interaction. When a nucleic acid binds to a target one, hydrogen bonds are the main component, therefore we evaluated hydrogen bonds between the antimiR or HDO-antimiR and miRNA (Figure 3). From these results, there was no difference in the frequency of binding between antimiR and HDO-antimiR. So, we analyzed the number and location of hydrogen bonds formed between antimiR and HDO-antimiR about Two-point or more interaction pattern to investigate the mechanism of the difference in effect between antimiR and HDO-antimiR.

In the Two-point interaction pattern about antimiR with miRNA, hydrogen bonds were formed mainly through the atoms in the base site of the antimiR and miRNA near both ends, and no hydrogen bonds were observed in the phosphate site and the sugar site of antimiR. Similar to antimiR, hydrogen bond was mainly observed at the base site in the miRNA (Figure 4a, Supplementary Table 1). In the Multiple-point interaction pattern about antimiR with miRNA, which was observed only once, hydrogen bonds were formed at the middle part of antimiR and miRNA, and there was no selectivity about the binding site in the residues of antimiR. Similar to Two-point interaction pattern, hydrogen bonds were observed mainly at the base site of the miRNA (Figure 4b, Supplementary Tables 1 and 3). HDO-antimiR was bound to miRNA at multiple points from 3' end of antimiR-strand (5' end of cRNA-strand) to the middle part of HDO-antimiR in the Two-point and Multiple-point interaction pattern. Importantly, hydrogen bonds between HDO-antimiR and miRNA were formed through the atoms in the phosphate site and the sugar site of HDO-antimiR, and no hydrogen bond was observed in the base site of the HDO-antimiR. In HDO-antimiR, cRNA-strand was mainly bound to miRNA and there was no difference in binding frequency depending on the type of RNA. On the other hand, guanine bases mainly formed hydrogen bonds in miRNA (Figure 4c and 4d, Supplementary Tables 2 and 3).

While most of the hydrogen bonds of antimiR are formed via the nucleobase, those of HDO-antimiR are formed via atoms at the phosphate site except for the both ends of antimiR-strand and cRNA-strand. Then we evaluated the time course of the hydrogen bonds in the simulations about Two-point interaction pattern of antimiR and Multiple-point interaction pattern of HDO-antimiR. When the simulation was performed up to 5 nsec, the number of hydrogen bonds increased up to 4 (Two-point interaction pattern) or 6 (Multiple-point interaction pattern) in each case. In antimiR, the site where hydrogen bonds are formed is initially abundant at the 5' end of the antimiR, and then the hydrogen bonds further increase around the 5' end of the antimiR with the passage of time (Figure 5a). On the other hand, in HDO-antimiR, the site where hydrogen bonds are formed is initially abundant at the 5' end of the c-RNA strand and miRNA, and then the hydrogen bonds gradually increase toward the 3' end of the miRNA with the passage of time, and we observed miRNA entwined with HDO-antimiR (Figure 5b). During the simulation, most of the hydrogen bonds on the HDO-antimiR were phosphate site, and the atoms in the base site were not observed except for some of the both ends of antimiR-strand and cRNA-strand (Figure 5b).

Difference in binding site at the binding of antimiR or HDO-antimiR and miRNA

Next, in order to perform simulation from a state in which antimiR or HDO-antimiR and miRNA are closer to each other, nucleic acids were placed 5 Å away to the vertical axis direction (Figure 6, Supplementary Figures 3 and 4), then miRNA was placed in the major groove of HDO-antimiR shifted to -5 Å from miRNA (Figure 6), or minor groove of HDO-antimiR shifted to +5 Å from miRNA (Supplementary Figure 4). It is unlikely that miRNA will fit in the minor groove of HDO-antimiR, which is a narrow and shallow groove, so we considered the pattern that fits in the deep major groove. In the case of antimiR and miRNA, most hydrogen bonds were formed between the bases of each other as similar to the case of 20 Å separation on the axial section of helix (Figure 6a, Supplementary Tables 4 and 5). Like antimiR, HDO-antimiR and miRNA formed hydrogen bonds via the atoms at the base of HDO-antimiR, not the phosphate site of the nucleic acid, unlike when they were separated by 20 Å on the axial section of helix (Figure 6b, Supplementary Tables 4 and 5).

We further analyzed these results about the Two-point interaction pattern and Multiple-point interaction pattern when antimiR or HDO-antimiR is 5 Å shifted from miRNA in the vertical axis direction (both miR122 and miR21). At first, to find out which sites contribute to nucleic acid binding, we calculated the number of hydrogen bonds confirmed in this simulation for each binding site in the nucleic acid (Figure 7a-d and Supplementary Figure 5). In these results, there are several types of interaction patterns between HDO-antimiR or antimiR and miRNA. The atoms in the base part mainly form hydrogen bonds in antimiR, whereas in HDO-antimiR, the atoms in the phosphate bond site are mainly involved. On the miRNA side, the atoms at the base were mainly bound either to antimiR or HDO-antimiR. It was also found that the appearance rate of the Multiple-point interaction pattern, which seems to be the strongest binding form, differs depending on the initial conditions between HDO-antimiR and antimiR and miRNA.

In the time course about Multiple-point interaction pattern of HDO-antimiR and miRNA showed hydrogen bonds were not fixed, and the atom that once formed a hydrogen bond with another atom, then HDO-antimiR bound to the target miRNA gradually. By repeating these movements, it was expected that the miRNA would entwine in the major groove of HDO-antimiR. On the other hand, when HDO-antimiR and miRNA were placed 5 Å away to the vertical axis direction, miRNA was placed in the major groove of HDO-antimiR in the initial state. In the result of this simulation, HDO-antimiR and miRNA formed hydrogen bonds via the atoms at the base of HDO-antimiR, not the phosphate site of the nucleic acid.

Next, in order to investigate which bases affect the binding, we calculated the number of hydrogen bonds for each base in the nucleic acid, then it was corrected by dividing by the number of each base in the sequence in order to eliminate the variation in the number of bases since the number of bases differs depending on the sequence (Figure 7e-h and Supplementary Figure 6). In the results about shifted 5 Å in the vertical axis direction, antimiR showed the number of hydrogen bonds between guanine and cytosine is larger than them between thymine and adenine. These results partly can reflect the fact that the number of hydrogen bonds between guanine and cytosine is 3 and the number of hydrogen bonds between thymine and adenine is 2 when antimiR and miRNA form a complete double strand. On the other hand, there was no difference in the number of hydrogen bonds depending on the base in HDO-antimiR. Binding site analyses showed HDO-antimiR and miRNA formed hydrogen bonds via the atoms at the base of HDO-antimiR, not the phosphate site of the HDO-antimiR when HDO-antimiR and miRNA were placed 5 Å away to the vertical axis direction, and these data suggested HDO-antimiR is bound to miRNA via a base, but it is bound by a mechanism different from that of antimiR and miRNA. These results indicated it is not affected by the base sequence in HDO-antimiR because not base site, but phosphate site affects the bond in HDO-antimiR.

Discussion

In MD simulation, all atoms that make up a nucleic acid molecule can be displayed in coordinates in XYZ space. MD simulation of HDO-antimiR or antimiR and the target miRNA at a distance of 20 Å separation on the axial section of helix confirmed that HDO-antimiR and antimiR bind to the target miRNA actually. It was also found that hydrogen bonds are important for binding, and computational studies have been useful in predicting and understanding molecular phenomena with H-bond interactions[19].

Our results show the simulations of 20 Å separation on the axial section of helix, representing the very early changes leading to the coupling, and the simulations of 5 Å separation to the vertical axis direction, representing the situation after the coupling has progressed. Nucleobases formed hydrogen bonds in the simulations about antimiR and miRNA both 20 Å separation and 5 Å separation. On the other hand, in the simulation about HDO-antimiR and miRNA, phosphate groups were mainly involved in the bond at 20 Å separation, while atoms at the base site were mainly involved in the bond at 5 Å separation. The result that the phosphate site of HDO-antimiR formed a hydrogen bond in 20 Å separation suggests that it binds in a sequence-independent manner. Since the base part formed a hydrogen bond in 5 Å separation, quence-dependent bond. This is a different

result from the simulation in the single-strand antimiR, and it is considered that it is a phenomenon peculiar to HDO-antimiR having a double-strand structure. In the sequence of miRNA, guanines had the largest effect on hydrogen bonds between antimiR or HDO-antimiR and miRNA. Compared to miR122, miR21 has a lower number of guanines in the sequence and it may be associated with a lower number of the bindings more than two-point interaction between antimiR and HDO-antimiR. The difference in the number of potential hydrogen bond acceptor sites and donor sites between guanine and other bases may have an effect.

There have been few reports about simulations of nucleic acid and target genes using molecular dynamics. Shen *et al.*[20] described the potential of estimating melting temperature for oligonucleotides including short interference RNA (siRNA) and ASO by using the standardized molecular dynamics protocol. In another report, Uppuladinne *et al.*[16] also described structural properties of ASO using molecular dynamics simulations in the duplex of ASO and its complementary RNA, and they evaluated binding energy of the duplex. But they mentioned about the influence of the several chemically modifications about ASO, and had only performed the simulation with ASO and its targeted RNA from the binding status. Therefore, unlike our reports, they did not evaluate how ASO binds to a target gene from a distant. Galindo-Murillo *et al.*[21] reported antisense inhibition by acyclic analogs of nucleic acids using molecular dynamics simulations, and they estimated the potentially identify target ASO analogs by root-mean-square (RMS) values. As just described, there are increasing reports on the function of antisense oligonucleotide using molecular dynamics because it is useful for functional evaluation of antisense nucleic acids.

Several proteins including plasma protein and intracellular protein affect pharmacokinetics of the phosphorothioate modified ASO[22], especially in the RNase H1-dependent ASO[23]. Recently we reported the identification of RNase H-dependent tocopherol-conjugated HDO interacting proteins[24]. Probably HDO-antimiR also have the interacting protein to affect to target miRNA, our results suggested that HDO-antimiR alone can bind to the target gene.

Our simulations were only in very short time, which is insufficient as a simulation of therapeutics oligonucleotide showing efficacy every few days, but new findings on how the nucleic acid binds to a target gene. In particular, it was suggested that the initial interaction with the target miRNA differs between the antimiR and the HDO-antimiR. In the future, if it becomes possible to simulate multiple and long-term oligonucleotide therapeutics with various proteins by using higher-performance computers including supercomputers, it is expected that more precise functions of therapeutic oligonucleotides will be verified.

Declarations

ACKNOWLEDGMENTS

This work was supported by Grant-in-Aid for JSPS Research Fellow (No.18J22727) from Japan Society for the Promotion of Science (JSPS), Japan. S.F. was supported by JSPS through the Program for Leading Graduate Schools (MERIT).

AUTHOR CONTRIBUTIONS

Designed the research, K.N., S.F., T.Y. and Y.S.; Performed the simulations, K.N. All authors wrote the manuscript.

DECLARATION OF INTERESTS

The authors declare no competing interests.

References

1. Ambros, V. The functions of animal microRNAs. *Nature*, **431**, 350–355 (2004).
2. Garzon, R., Marcucci, G. & Croce, C. M. Targeting microRNAs in cancer: rationale, strategies and challenges. *Nat. Rev. Drug Discov*, **9**, 775–789 (2010).
3. Rupaimoole, R. & Slack, F. J. MicroRNA therapeutics: towards a new era for the management of cancer and other diseases. *Nat. Rev. Drug Discov*, **16**, 203–222 (2017).
4. Krützfeldt, J. *et al.* Silencing of microRNAs in vivo with 'antagomirs'. *Nature*, **431**, 685–689 (2004).
5. Hara, R. I., Yoshioka, K. & Yokota, T. DNA-RNA heteroduplex oligonucleotide for highly efficient gene silencing. *Methods Mol. Biol*, **2176**, 113–119 (2020).
6. Nishina, K. *et al.*. DNA/RNA heteroduplex oligonucleotide for highly efficient gene silencing. *Nat. Commun*, **6**, 1–13 (2015).
7. Kuwahara, H. *et al.* Modulation of blood-brain barrier function by a heteroduplex oligonucleotide in vivo. *Sci. Rep*, **8**, 1–12 (2018).
8. Lei, Mon, S. S. *et al.* Highly efficient gene silencing in mouse brain by overhanging-duplex oligonucleotides via intraventricular route. *FEBS Lett*, **594**, 1413–1423 (2020).
9. Nagata, T. *et al.* Cholesterol-functionalized DNA/RNA heteroduplexes cross the blood–brain barrier and knock down genes in the rodent CNS.*Nat. Biotechnol.*https://pubmed.ncbi.nlm.nih.gov/34385691/ (2021).
10. Yoshioka, K. *et al.* Highly efficient silencing of microRNA by heteroduplex oligonucleotides. *Nucleic Acid Res*, **47**, 7321–7332 (2019).
11. Suzuki, M. *et al.* Effective silencing of miR-126 after ischemic stroke by means of intravenous α-tocopherol–conjugated heteroduplex oligonucleotide in mice. *Sci. Rep*, **11**, 14237 (2021).
12. Shibuta, Y. *et al.* Heterogeneity in homogeneous nucleation from billion-atom molecular dynamics simulation of solidification of pure metal. *Nat. Commun*, **8**, 10 (2017).

13. Maekawa, Y., Shibuta, Y. & Sakata, T. Effect of double-stranded DNA on electrical double layer structure at oxide/electrolyte interface in classical molecular dynamics simulation. *Chem. Phys. Lett*, **619**, 152–157 (2015).
14. Salomon-Ferrer, R., Case, D. A. & Walker, R. C. An overview of the Amber biomolecular simulation package. *WIREs Comput. Mol. Sci*, **3**, 198–210 (2013).
15. Case, D. A. *et al.* The Amber biomolecular simulation programs. *J. Computat. Chem*, **26**, 1668–1688 (2005).
16. Uppuladinne, M. V. N., Sonavane, U. B., Deka, R. C. & Joshi, R. R. Structural insight into antisense gapmer-RNA oligomer duplexes through molecular dynamics simulations. *J. Biomol. Struct. Dyn*, **40**, 2823–2836 (2019).
17. Iwamoto, N. *et al.* Control of phosphorothioate stereochemistry substantially increases the efficacy of antisense oligonucleotides. *Nat. Biotechnol*, **35**, 845–851 (2017).
18. Østergaard, M. E. *et al.* Understanding the effect of controlling phosphorothioate chirality in the DNA gap on the potency and safety of gapmer antisense oligonucleotides. *Nucleic Acids Res*, **48**, 1691–1700 (2020).
19. Jayaraman, A. & 100th Anniversary of Macromolecular Science Viewpoint. Modeling and simulation of macromolecules with hydrogen bonds: challenges, successes, and opportunities. *ACS Macro Lett*, **9**, 656–665 (2020).
20. Shen, L. *et al.* Molecular dynamics simulation and binding energy calculation for estimation of oligonucleotide duplex thermostability in RNA-based therapeutics. *J. Chem. Inf. Model*, **51**, 1957–1965 (2011).
21. Galindo-Murillo, R., Cohen, J. S. & Akabayov, B. Molecular dynamics simulations of acyclic analogs of nucleic acids for antisense inhibition. *Mol. Ther. Nucleic Acids*, **23**, 527–535 (2021).
22. Crooke, S. T., Vickers, T. A. & Liang, X. Phosphorothioate modified oligonucleotide–protein interactions. *Nucleic Acids Res*, **48**, 5235–5253 (2020).
23. Lingdi, Z., Vickers, T. A., Sun, H., Liang, X. & Crooke, S. T. Binding of phosphorothioate oligonucleotides with RNase H1 can cause conformational changes in the protein and alter the interactions of RNase H1 with other proteins. *Nucleic Acids Res*, **49**, 2721–2739 (2021).
24. Asada, K. *et al.* Short DNA/RNA heteroduplex oligonucleotide interacting proteins are key regulators of target gene silencing. *Nucleic Acids Res*, **49**, 4864–4876 (2021).

Tables

Table 1. The sequences and chemically modification of the antimiR or HDO-antimiR and targeting miRNA (miR-122)

antimiR (5 → 3)	miRNA (5 → 3)
LC1	U16
DC2	G17
LA3	G18
DT4	A19
DT5	G20
LG6	U21
LT7	G22
DC8	U23
DA9	G24
LC10	A25
DA11	C26
LC12	A27
DT13	A28
LC14	U29
LC15	G30
	G31
	U32
	G33
	U34
	U35
	U36
	G37
	U38

HDO		miRNA (5 → 3)
antimiR-strand (5 → 3)	cRNA-strand (5 → 3)	
LC1	G16	U31
DC2	G17	G32
LA3	A18	G33
DT4	G19	A34
DT5	U20	G35
LG6	G21	U36
LT7	U22	G37
DC8	G23	U38
DA9	A24	G39
LC10	C25	A40
DA11	A26	C41
LC12	A27	A42
DT13	U28	A43
LC14	G29	U44
LC15	G30	G45
		G46
		U47
		G48
		U49
		U50
		U51
		G52
		U53

LX: LNA, DX: DNA, X: RNA
G: Guanine, A: Adenine, U: Uracil, T: Thymine, C: Cytosine
LC: 5-Methylcytosine LNA
Internucleotide linkage: phosphorothioate in the antimiR and antimiR-strand of HDO-antimiR, phosphodiester in the miRNA and cRNA-strand of HDO-antimiR

Figures

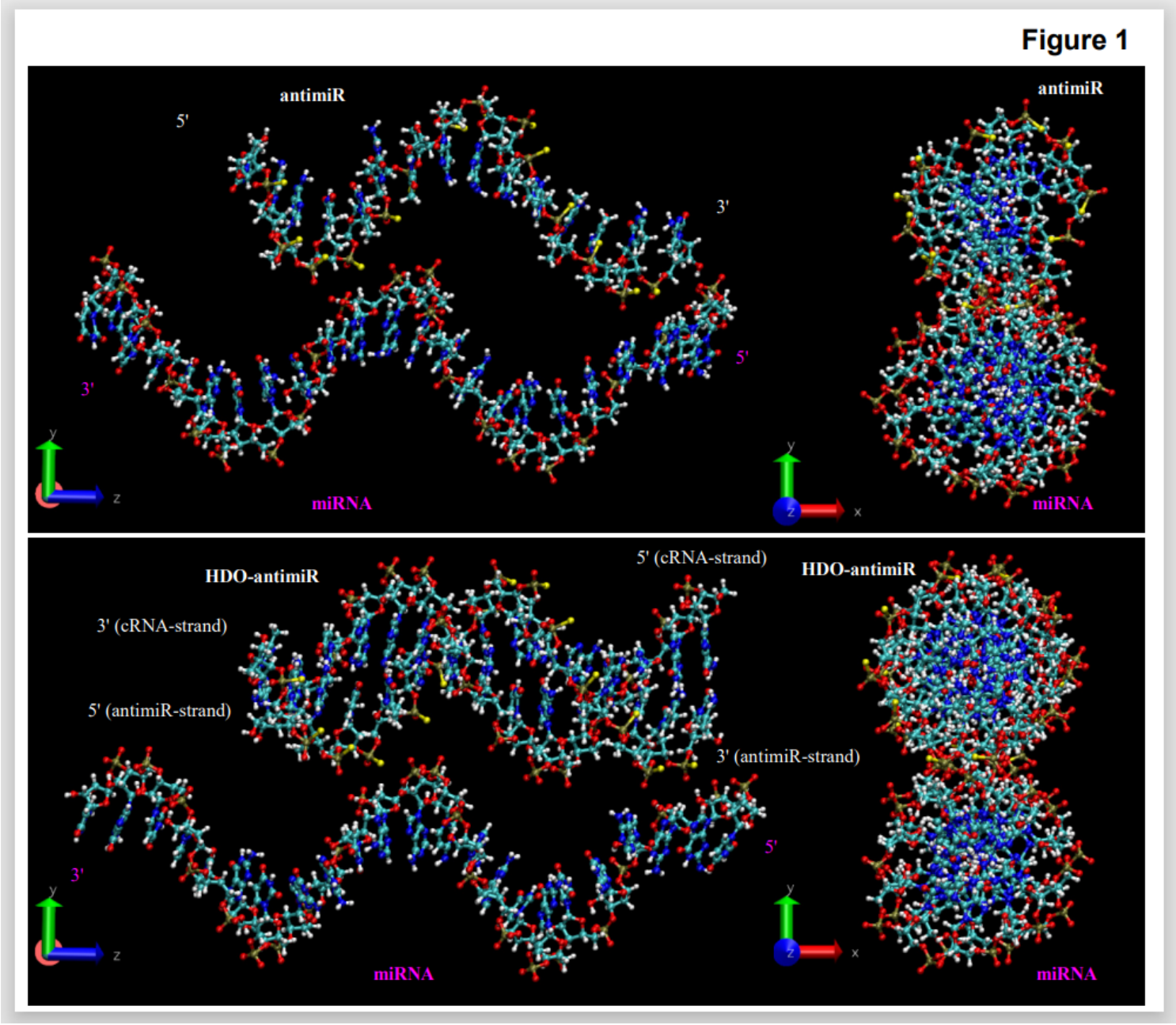

Figure 1

Initial structure of miR122 (single strand) and antimiR122 (single strand) or HDO-antimiR122 (double strand). White: H, Red: O, Light blue: C, Blue: N, Gold: P, Yellow: S

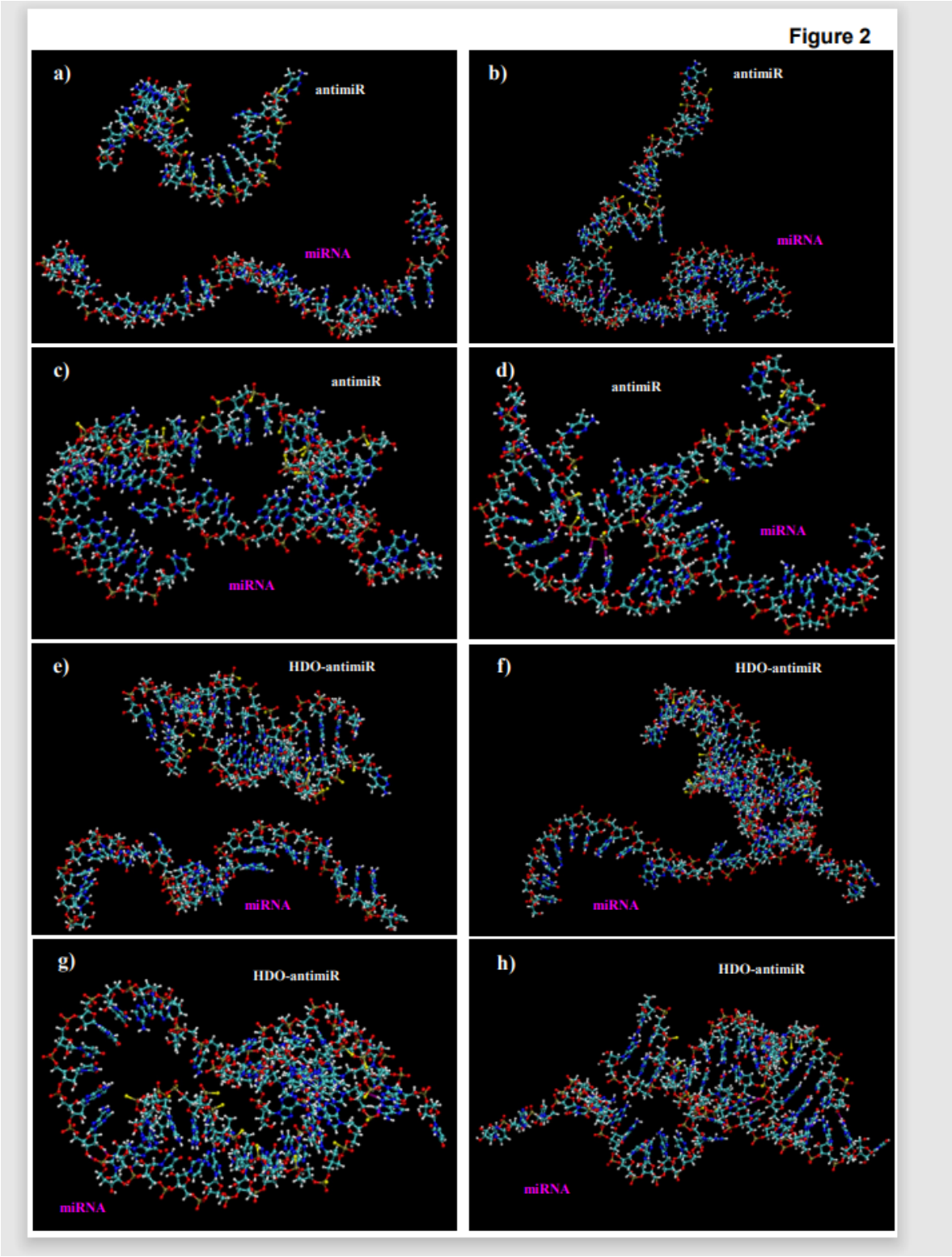

Figure 2

Various patterns of structure about antimiR or HDO-antimiR and miRNA at final step. a) antimiR122; No interaction pattern, b) antimiR122; One-point interaction pattern, c) antimiR122; Two-point interaction pattern, d) antimiR122; Multiple-point interaction pattern, e) HDO-antimiR122; No interaction pattern, f) HDO-antimiR122; One-point interaction pattern, g) HDO-antimiR21; Two-point interaction pattern, h) HDO-

ed: O, Light blue: C, Blue: N, Gold: P, Yellow: S,

Magenta: Hydrogen bonds between antimiR or HDO-antimiR and miRNA (The hydrogen bonds are indicated by dashed lines)

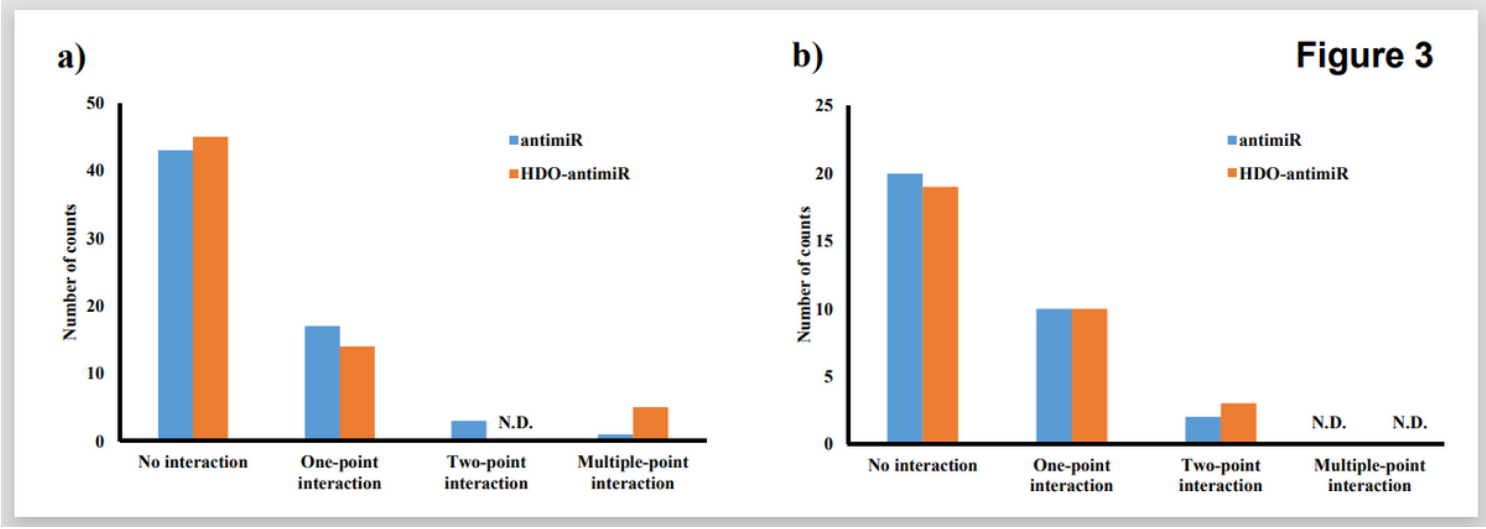

Figure 3

Frequency of several types of structure at final step between antimiR or HDO-antimiR and targeted miRNA. a) miR122 (n = 64). N.D., not detected. b) miR21 (n = 32). N.D., not detected.

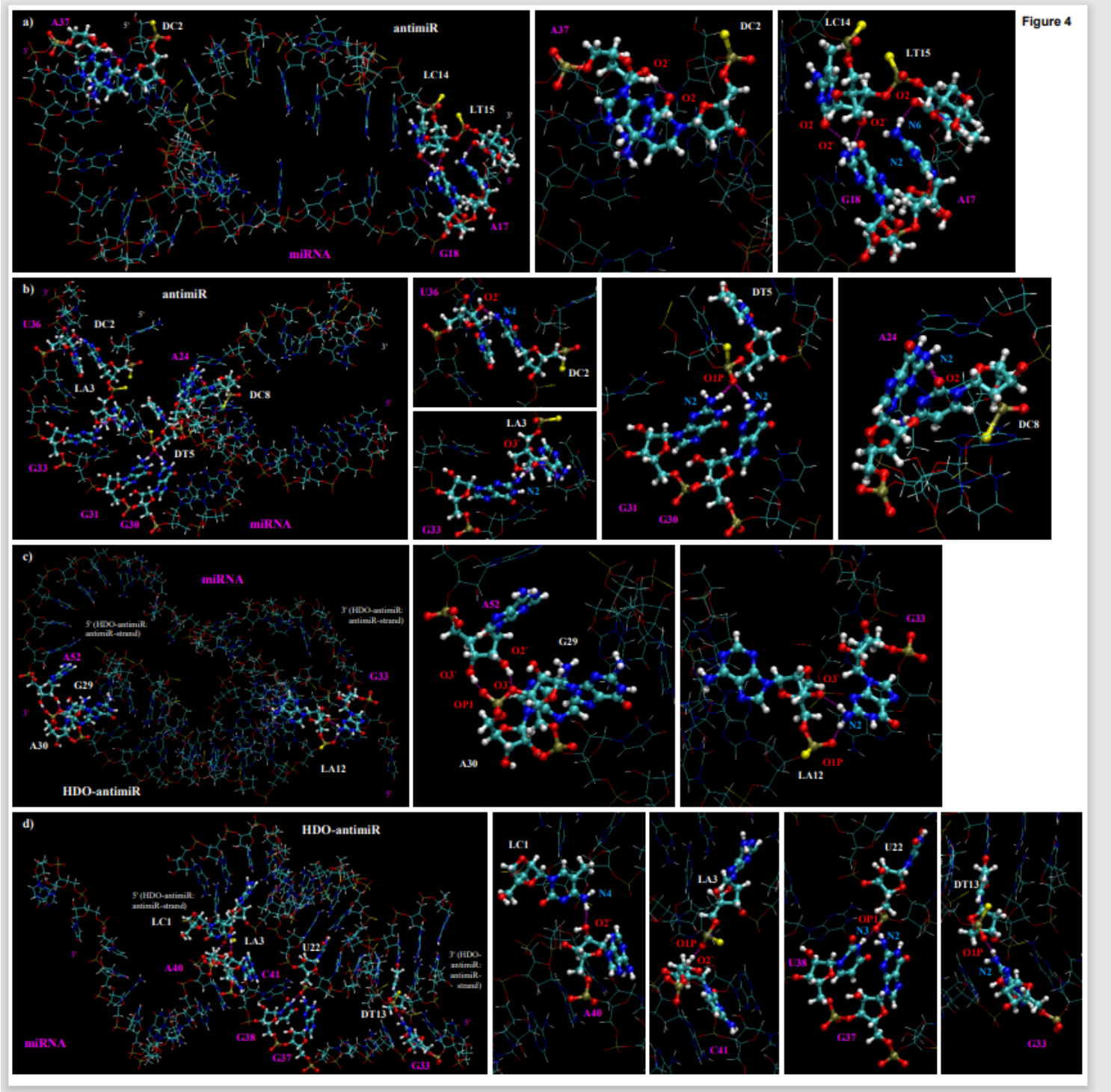

Figure 4

Effect of hydrogen bond in Two-point and Multiple-point interaction pattern. a) antimiR21; Two-point interaction pattern, b) antimiR122; Multiple-point interaction pattern, c) HDO-antimiR21; Two-point interaction pattern, d) HDO-antimiR122; Multiple-point interaction pattern White: H, Red: O, Light blue: C, Blue: N, Gold: P, Yellow: S, Magenta: Hydrogen bonds between antimiR or HDO-antimiR and miRNA (The hydrogen bonds are indicated by dashed lines)

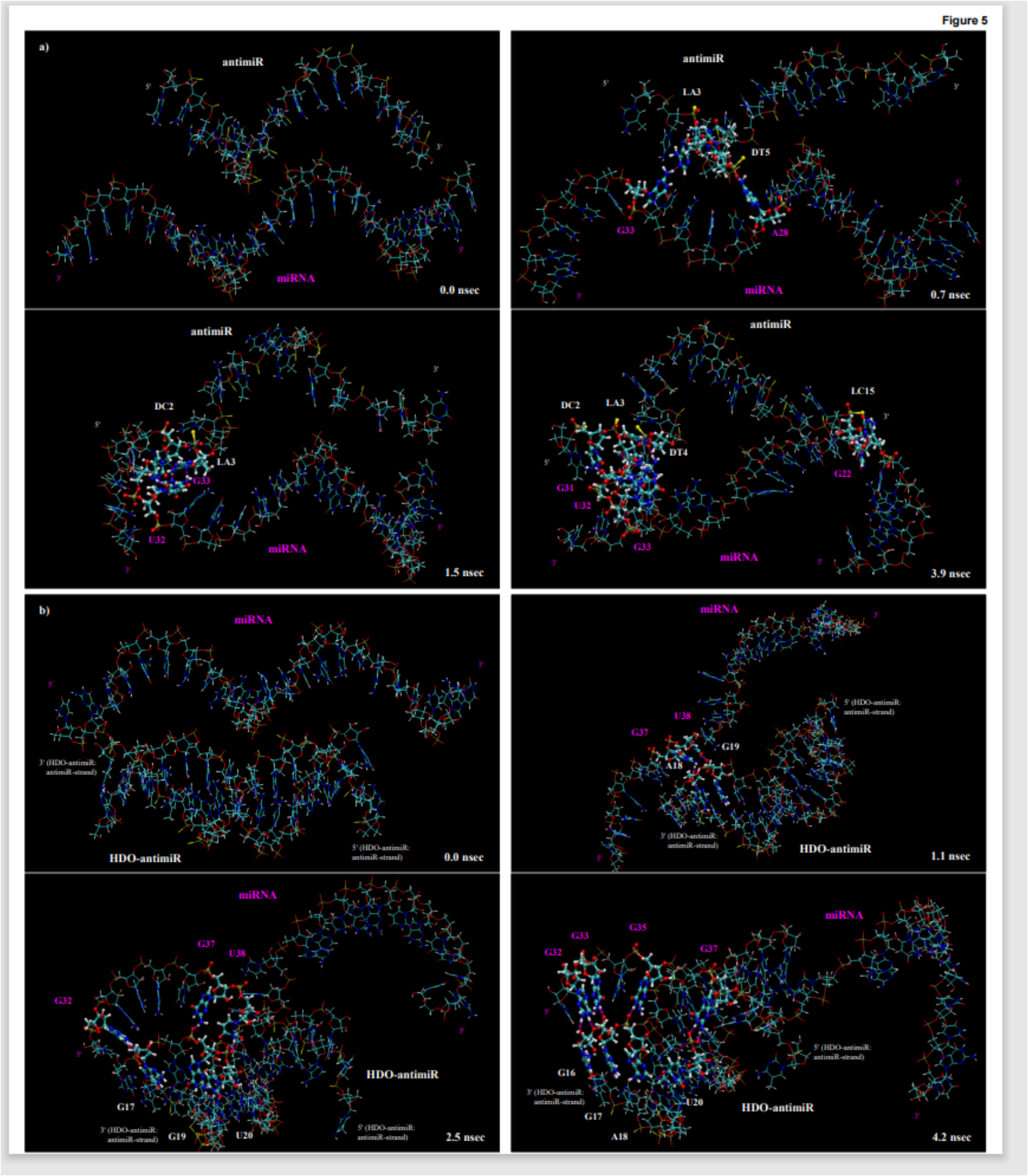

Figure 5

Time course of Two-point interaction pattern between antimiR and miRNA or Multiple-point interaction pattern between HDO-antimiR and miRNA a) antimiR122; Two-point interaction pattern, b) HDO-antimiR122; Multiple-point interaction pattern White: H, Red: O, Light blue: C, Blue: N, Gold: P, Yellow: S, Magenta: Hydrogen bonds between antimiR or HDO-antimiR and miRNA (The hydrogen bonds are

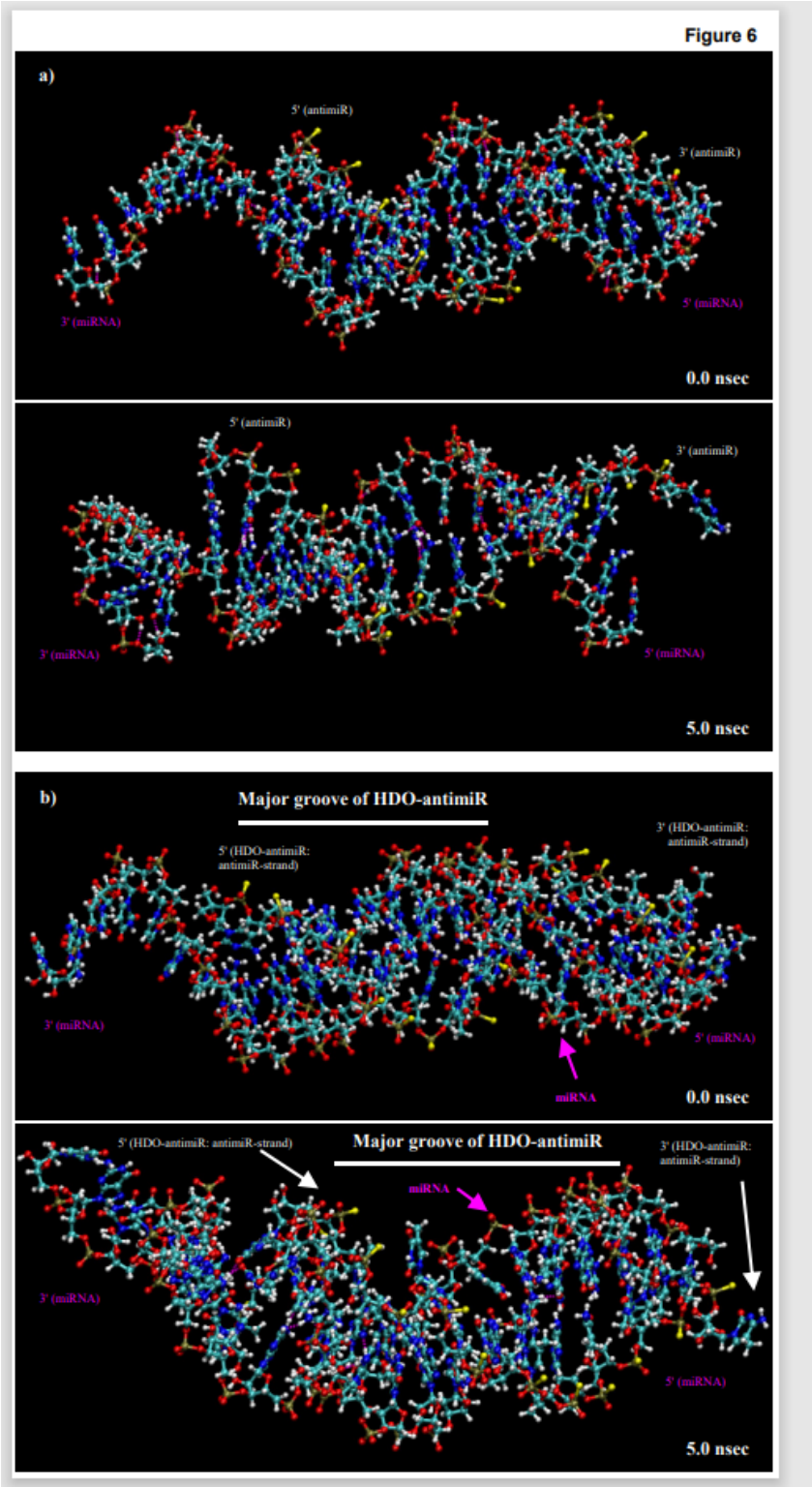

Figure 6

Shift antimiR122 or HDO-antimiR122 from miR122 -5 Å away to the vertical axis direction, initial state (0 nsec) and final step (5 nsec). a) antimiR122, b) HDO-antimiR122 White: H, Red: O, Light blue: C, Blue: N, Gold: P, Yellow: S, Magenta: Hydrogen bonds between antimiR or HDO-antimiR and miRNA (The hydrogen bonds are indicated by dashed lines)

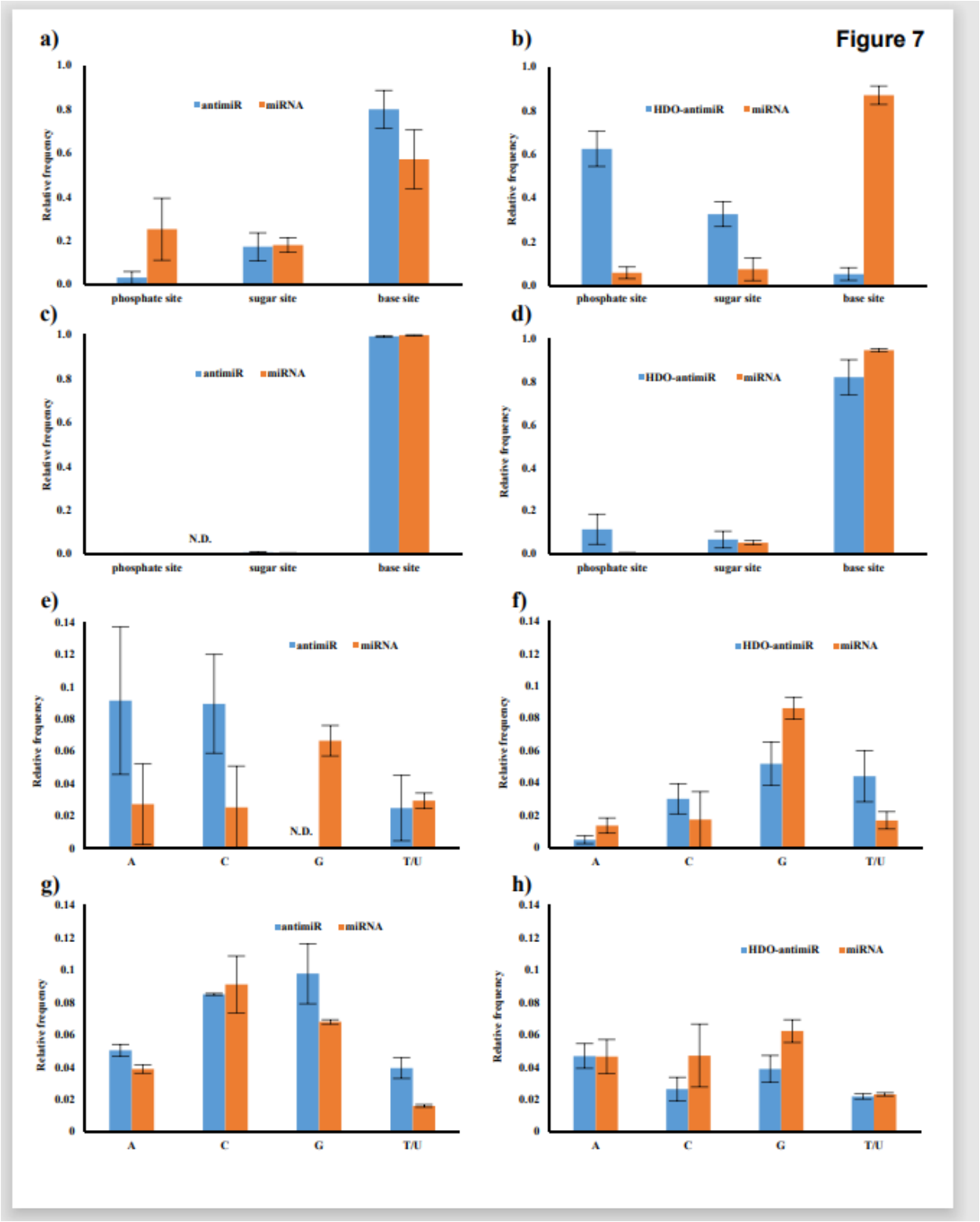

Figure 7

Analyses about binding site (a-d) or base site (e-h) of the number of hydrogen bonds between HDO-antimiR122 or antimiR122 and miR122. a) antimiR122; 20 Å shifted from miR122 in the horizontal section, Two-point interaction pattern. The results are presented as mean ± SEM (n = 3). b) HDO-antimiR122; 20 Å shifted from miR122 in the horizontal section, Multiple-point interaction pattern. The

22; -5 Å shifted from miR122 in the sagittal

direction. The results are presented as mean ± SEM (n = 3). N.D., not detected. d) HDO-antimiR122; -5 Å shifted from miR122 in the sagittal direction. The results are presented as mean ± SEM (n = 3). e) antimiR122; 20 Å shifted from miR122 in the horizontal section, Two-point interaction pattern. The results are presented as mean ± SEM (n = 3). N.D., not detected. f) HDO-antimiR122; 20 Å shifted from miR122 in the horizontal section, Multiple-point interaction pattern. The results are presented as mean ± SEM (n = 5). g) antimiR122; -5 Å shifted from miR122 in the sagittal direction. The results are presented as mean ± SEM (n = 3). h) HDO-antimiR122; -5 Å shifted from miR122 in the sagittal direction. The results are presented as mean ± SEM (n = 3).

Supplementary Files

This is a list of supplementary files associated with this preprint. Click to download.

- SupInfoHQ.pdf